

Supporting Information

Temperature-Guided Solidification of Copper Coordination Complexes as Hole Transport Materials

Timo Keller,^a Iacopo Benesperi,^{a,b} Jakob Thyr,^c Tomas Edvinsson,^c Elizabeth A. Gibson,^a and Marina Freitag^{a,*}

^a School of Natural and Environmental Science, Bedson Building, Newcastle University, NE1 7RU, Newcastle upon Tyne, UK. E-mail: marina.freitag@newcastle.ac.uk

^b University of Turin, Department of Chemistry, NIS Interdepartmental Centre and INSTM Reference Centre, Via Quarelo 15/A, 10135 Torino (TO), Italy

^c Department of Materials Science and Engineering, Solid State Physics, Ångström Laboratory, Uppsala University, Box 35, 751 03, Uppsala, Sweden

Contents

1 Results and Discussion	II
1.1 Photovoltaic Performance	II
1.2 Morphology	IV
1.3 Charge Collection and Transfer	VIII
1.4 Transient Measurements	X
1.5 Spectroscopy	XIII
1.6 Impedance Spectroscopy	XIV

1 Results and Discussion

1.1 Photovoltaic Performance

1 sun/50 °C	V _{OC} (mV)	J _{SC} (mA cm ⁻²)	FF (%)	PCE (%)	Info
Liquid EL	1044	12.77	75.5	10.07	
2 min	1044	12.14	75.8	9.65	
10 min	1037	11.20	75.6	8.78	
20 min	1043	12.38	75.2	9.74	
30 min	1023	10.07	74.5	7.87	
60 min	1032	12.43	75.1	9.63	15% discard

Ambient/50 °C	V _{OC} (mV)	J _{SC} (μ A cm ⁻²)	FF (%)	PCE (%)	Info
Liquid EL	876	75.06	77.1	15.27	
2 min	881	76.02	76.6	15.59	
10 min	881	71.57	74.8	14.28	
20 min	861	71.92	73.1	13.74	
30 min	865	70.31	74.2	13.65	
60 min	832	68.95	72.9	12.81	15% discard

Table S1 Performance metrics for the solid-state formation process under 50 °C for 100 mW cm⁻² solar irradiance (top) and 1000 lux ambient conditions (bottom).

1 sun/90 °C	V _{OC} (mV)	J _{SC} (mA cm ⁻²)	FF (%)	PCE (%)	Info
Liquid EL	1042	12.80	72.9	9.72	
2 min	1040	9.37	72.3	7.26	20% discard
10 min	-	-	-	-	100% discard

Ambient/90 °C	V _{OC} (mV)	J _{SC} (μ A cm ⁻²)	FF (%)	PCE (%)	Info
Liquid EL	829	72.48	74.6	13.43	
2 min	781	55.34	71.3	9.58	20% discard
10 min	-	-	-	-	100% discard

Table S2 Performance metrics for the solid-state formation process under 90 °C for 100 mW cm⁻² solar irradiance (top) and 1000 lux ambient conditions (bottom).

1 sun/110 °C	V _{OC} (mV)	J _{SC} (mA cm ⁻²)	FF (%)	PCE (%)	Info
Liquid EL	1020	12.43	74.1	9.41	
2 min	-	-	-	-	100% discard

Ambient/110 °C	V _{OC} (mV)	J _{SC} (μ A cm ⁻²)	FF (%)	PCE (%)	Info
Liquid EL	827	69.7	82.6	14.85	
2 min	-	-	-	-	100% discard

Table S3 Performance metrics for the solid-state formation process under 110 °C for 100 mW cm⁻² solar irradiance (top) and 1000 lux ambient conditions (bottom).

1 sun/tBP	V _{OC} (mV)	J _{SC} (mA cm ⁻²)	FF (%)	PCE (%)	Info
Liquid EL	1037	12.56	74.7	9.73	
2 weeks	942	11.78	74.5	8.27	65% discard

Ambient/tBP	V _{OC} (mV)	J _{SC} (μ A cm ⁻²)	FF (%)	PCE (%)	Info
Liquid EL	827	69.7	82.6	14.85	
2 weeks	769	62.5	76.7	10.73	65% discard

Table S4 Performance metrics for the solid-state formation process after 2 weeks for 100 mW cm⁻² solar irradiance (top) and 1000 lux ambient conditions (bottom) using tBP as the base.

1 sun/NMBI	V _{OC} (mV)	J _{SC} (mA cm ⁻²)	FF (%)	PCE (%)	Info
Liquid EL	1039	13.06	74.9	10.17	
2 weeks	999	10.93	72.8	7.94	75% discard

Ambient/NMBI	V _{OC} (mV)	J _{SC} (μ A cm ⁻²)	FF (%)	PCE (%)	Info
Liquid EL	878	72.3	80.8	15.69	
2 weeks	765	58.6	76.9	10.03	75% discard

Table S5 Performance metrics for the solid-state formation process after 2 weeks for 100 mW cm⁻² solar irradiance (top) and 1000 lux ambient conditions (bottom) using NMBI as the base.

1 sun/50 °C	V _{OC} (mV)	J _{SC} (mA cm ⁻²)	FF (%)	PCE (%)	Info
Liquid EL	1052	12.41	75.0	9.79	
10 min/Vac	1023	4.68	71.9	3.53	75% discard
30 min/Vac	991	3.51	73.5	2.48	90% discard

Ambient/50 °C	V _{OC} (mV)	J _{SC} (μ A cm ⁻²)	FF (%)	PCE (%)	Info
Liquid EL	845	73.3	79.3	14.56	
10 min/Vac	845	63.6	75.1	11.92	75% discard
30 min/Vac	819	64.5	75.7	11.76	90% discard

Table S6 Performance metrics for the solid-state formation process under 50 °C and Vacuum for 100 mW cm⁻² solar irradiance (top) and 1000 lux ambient conditions (bottom).

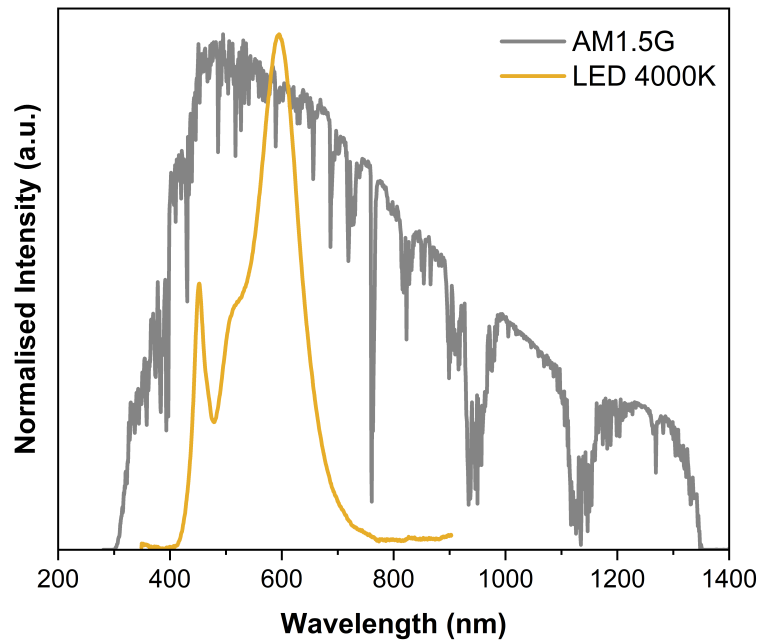


Figure S1 Normalised spectra of the AM1.5G spectra (gray) for outdoor measurements and the measured LED 4000K spectra (yellow) for the indoor characterisation.

1.2 Morphology

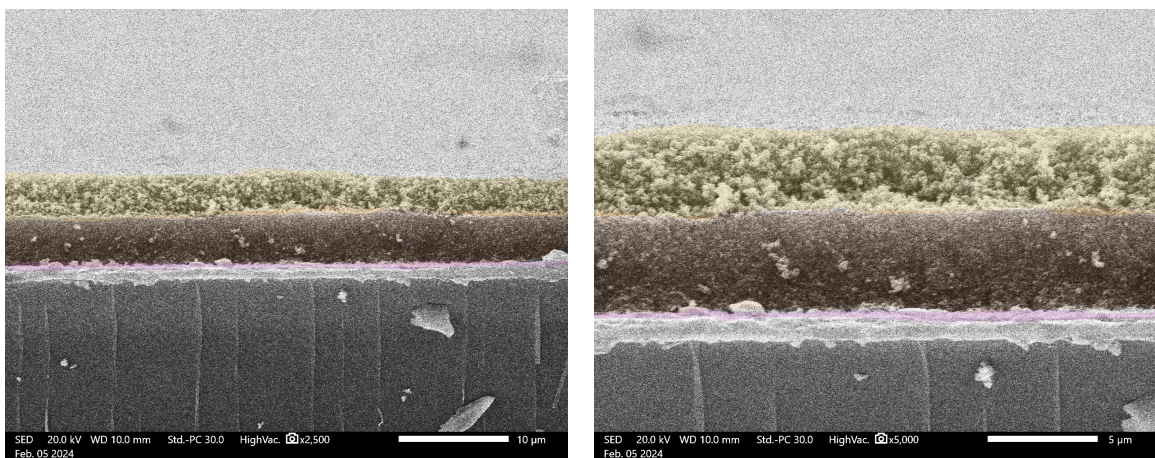


Figure S2 Cross-sectional SEM image of the dye on titania layer at 2500x (left) and 5000x (right) magnification.

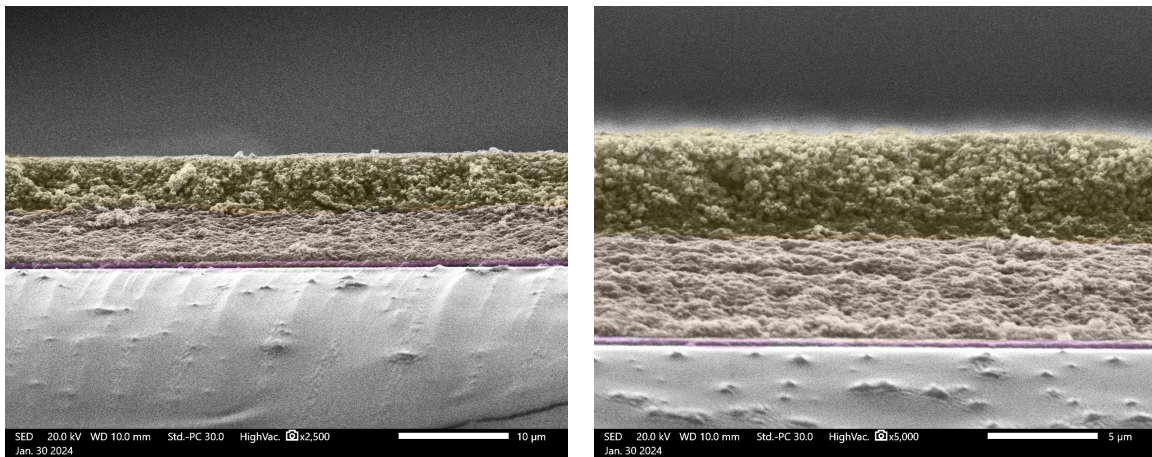


Figure S3 Cross-sectional SEM image of the liquid-junction dye-sensitised solar cell at 2500x (left) and 5000x (right) magnification.

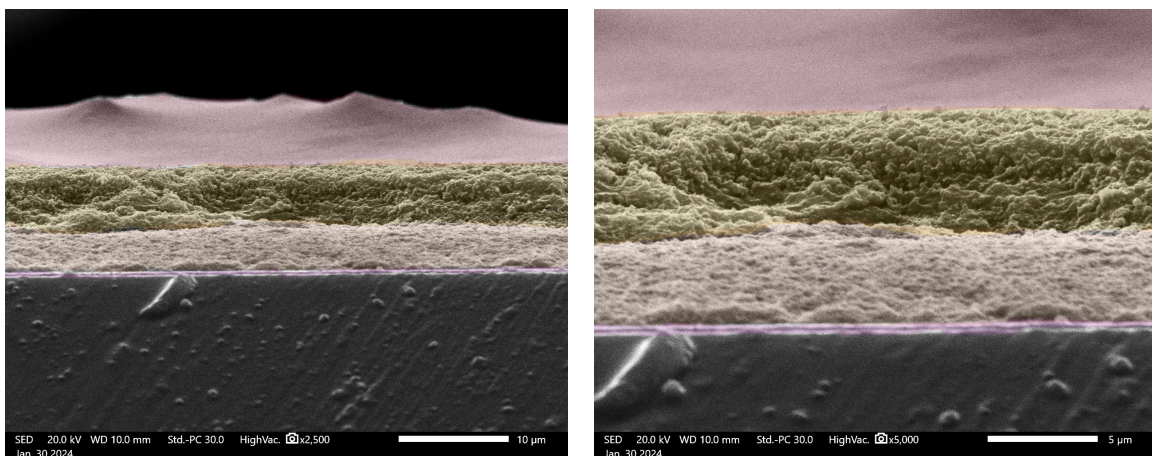


Figure S4 Cross-sectional SEM image of the solid-state cell at 2500x (left) and 5000x (right) magnification after the solid-state formation process at 70 °C.

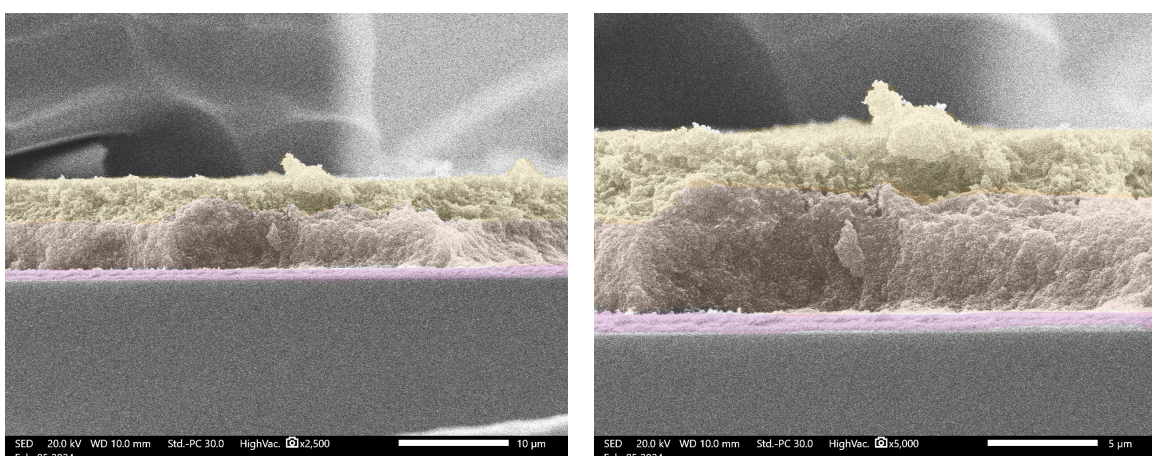


Figure S5 Cross-sectional SEM image of the drop-cased HTM at 2500x (left) and 5000x (right) magnification.

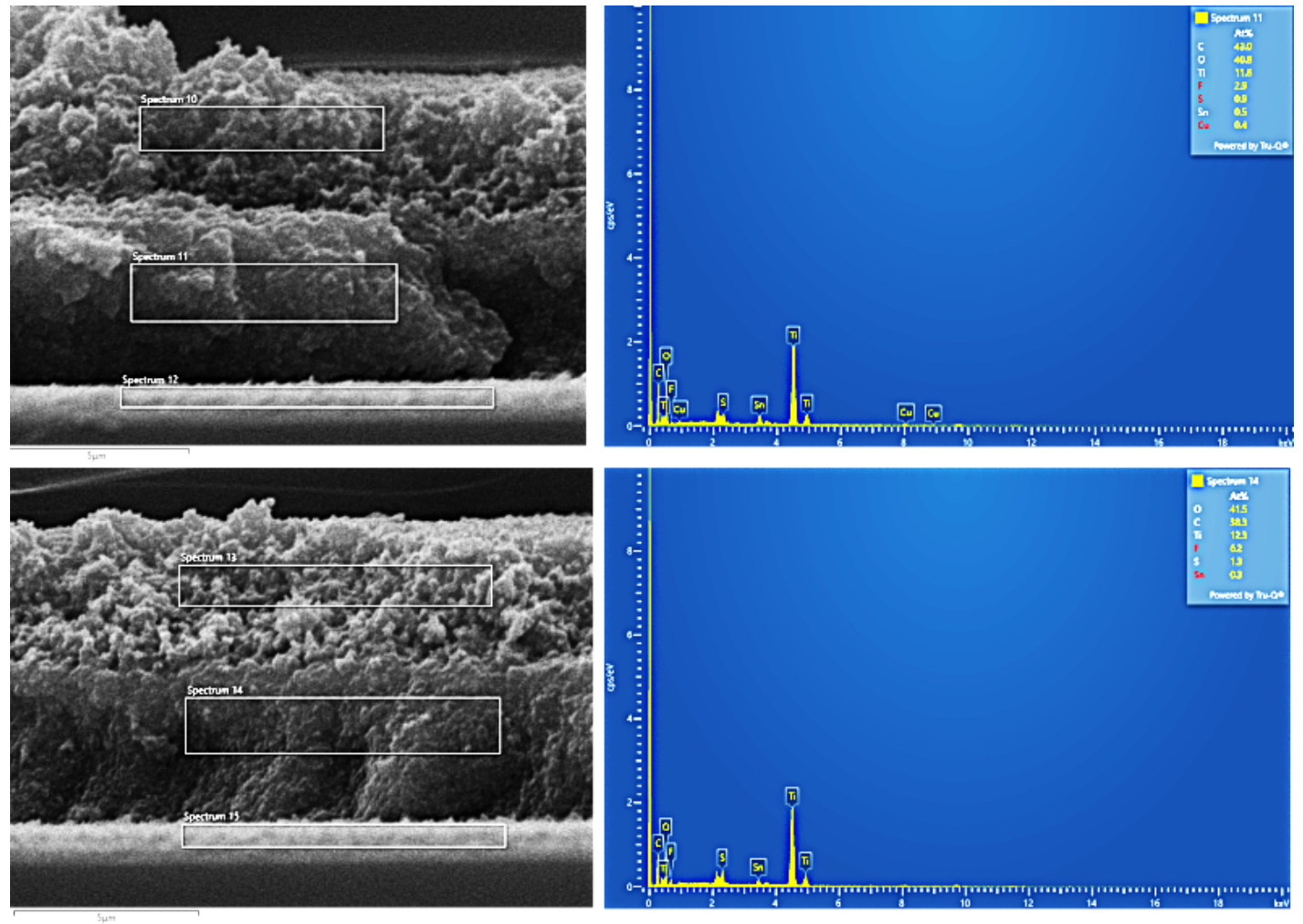


Figure S6 EDX analysis of mesoporous layer with HTM via solid-state formation process (top) and drop-casting (bottom).

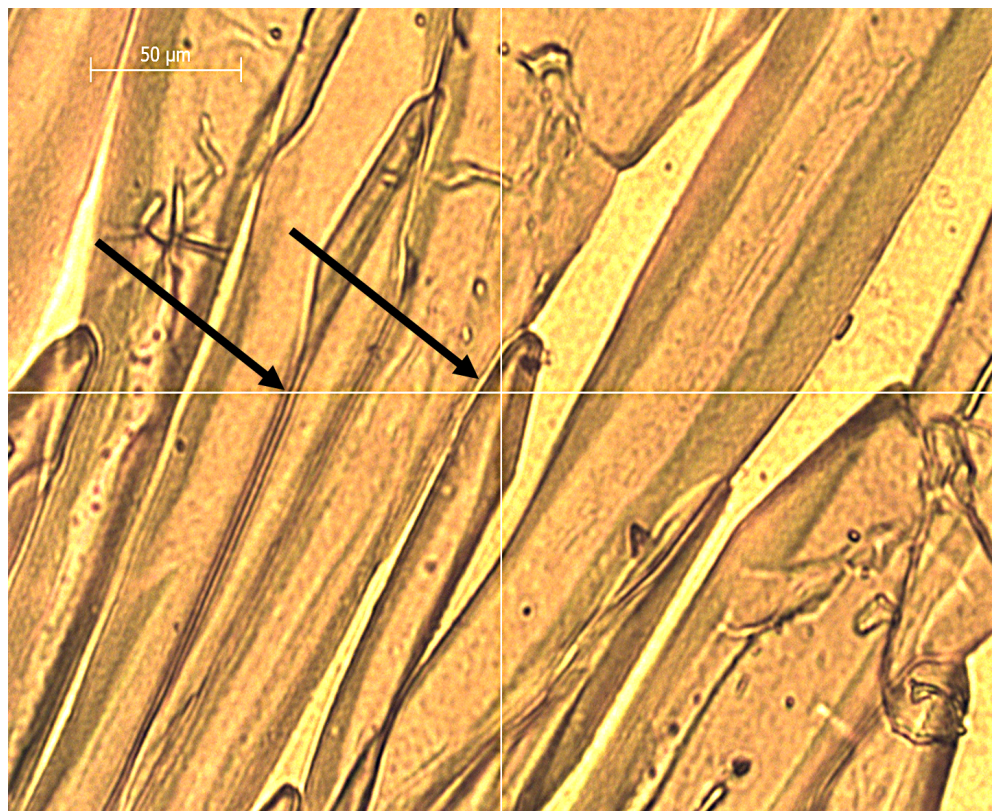


Figure S7 Microscopy image of the crystal growth of the Cu(tmby)₂TFSI_{1/2} on TiO₂, induced by high temperature solid-state formation conditions. The arrows indicate grain boundaries.

1.3 Charge Collection and Transfer

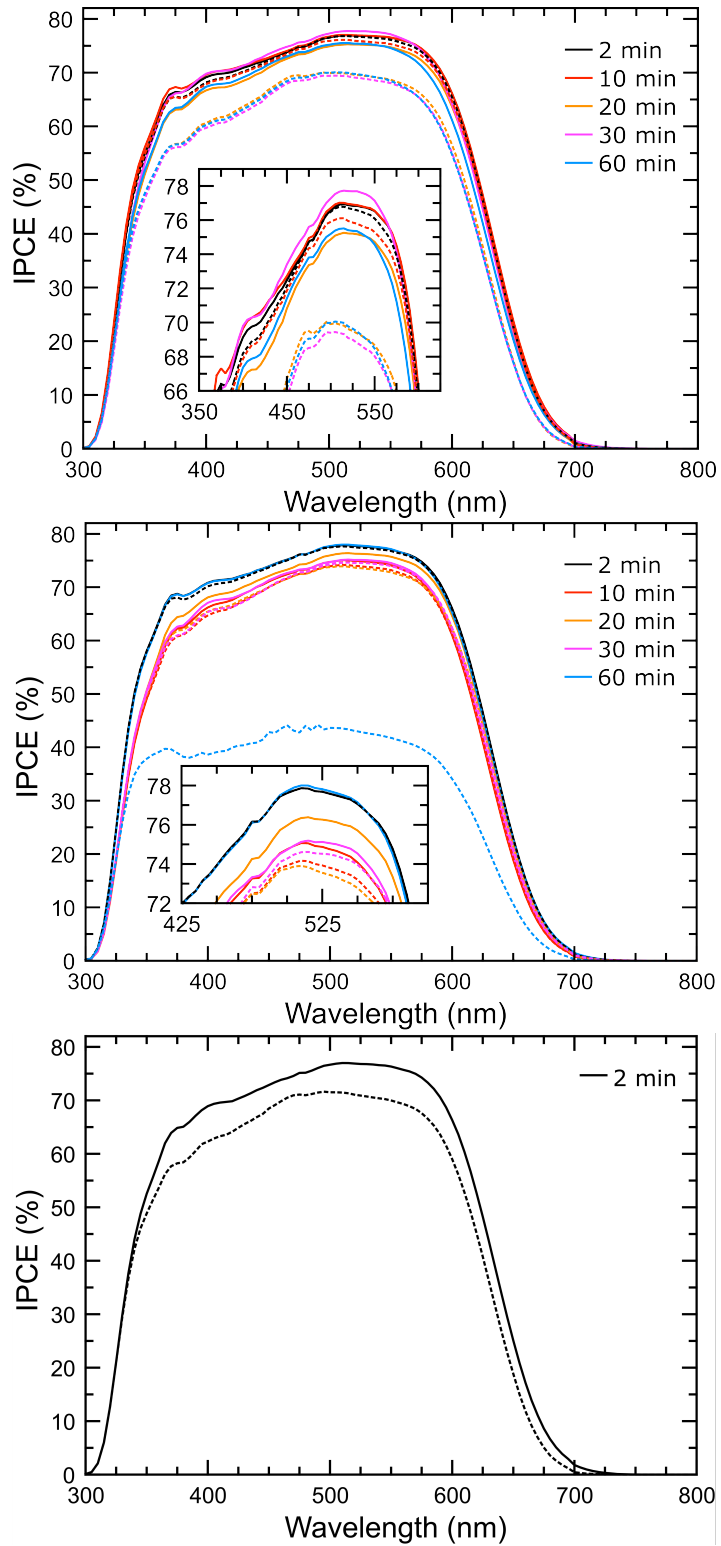


Figure S8 Incident-photon-to-current efficiencies before (solid line) and after (dotted line) the solid-state formation process at 50 °C (top), 70 °C (middle) and 90 °C (bottom).

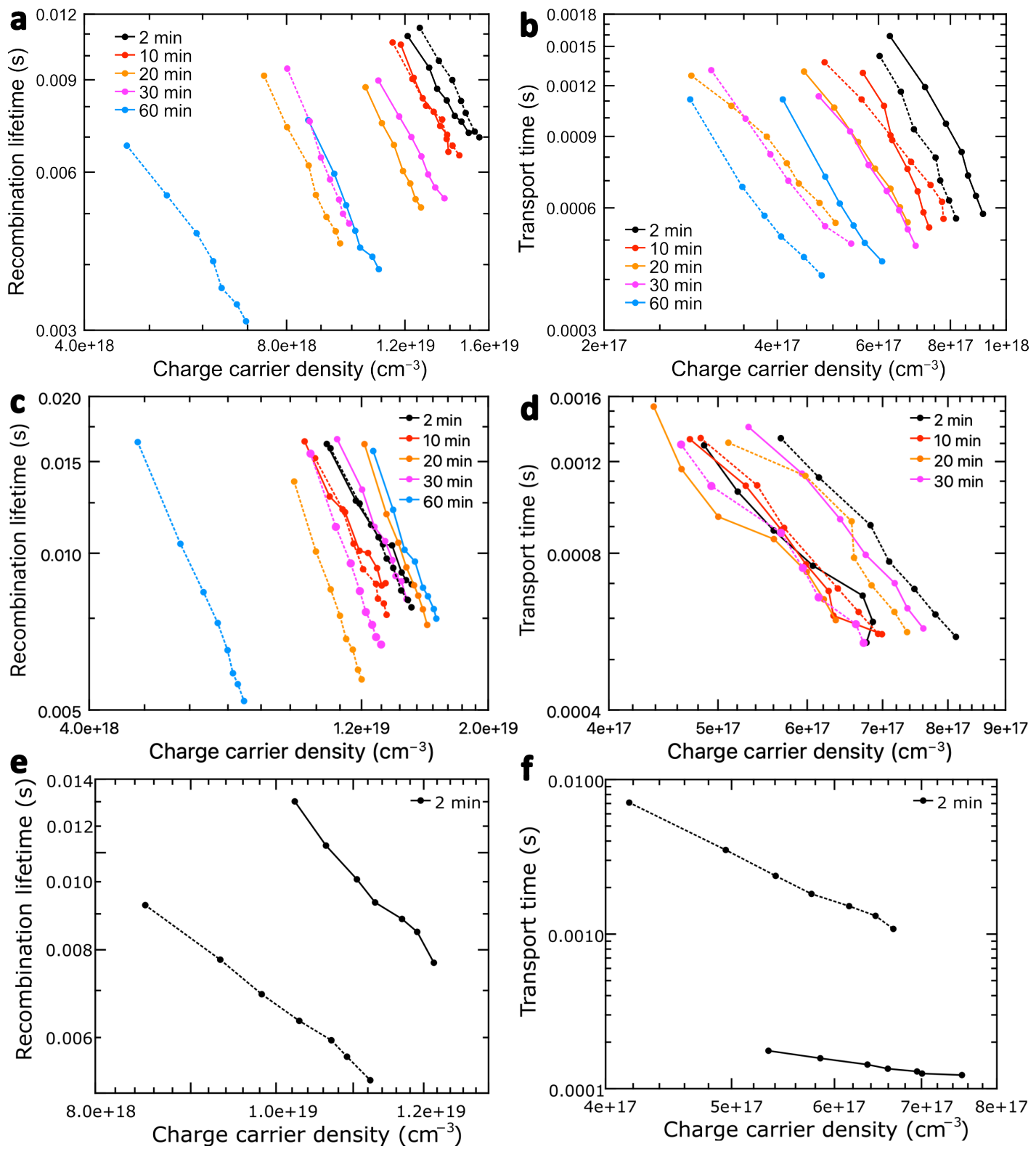


Figure S9 Electron lifetime a), c), e) and transport time b), d), f) before (solid line) and after (dotted line) the solid-state formation process at a), b) at 50°C, c), d) at 70°C, e), f) at 90°C.

1.4 Transient Measurements

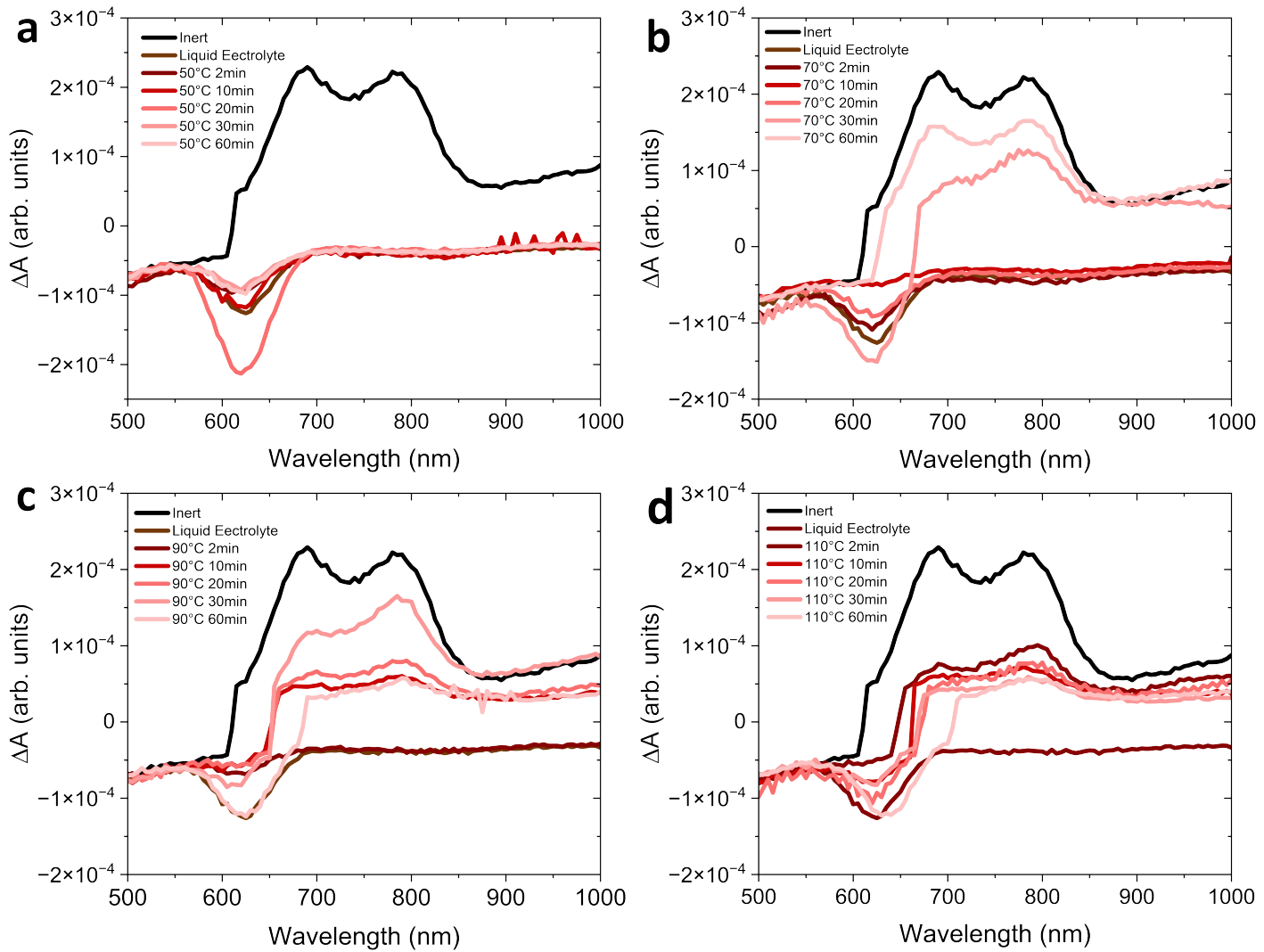


Figure S10 Photoinduced absorption spectroscopy (PIA) before and after the solid-state formation process at a) 50°C, b) 70°C, c) 90°C and d) 110°C.

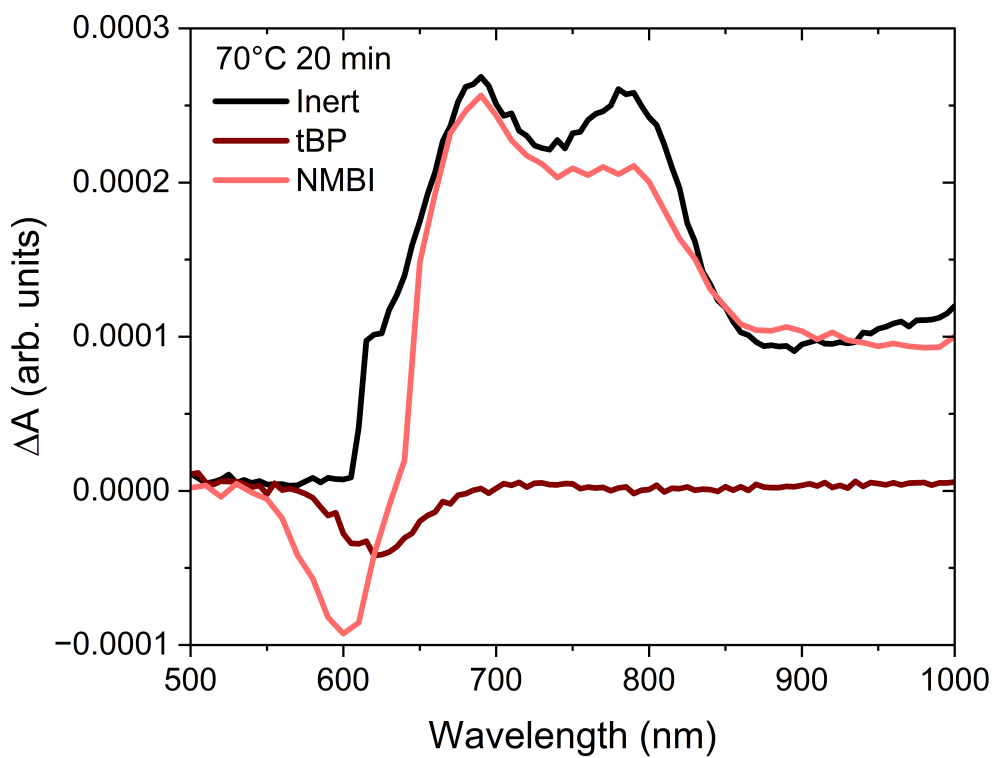


Figure S11 Comparison of the photoinduced absorption spectroscopy (PIA) signals of samples with tBP and NMBI bases in the electrolyte after heat treatment at 70 °C for 20 minutes, in relation to the inert electrolyte.

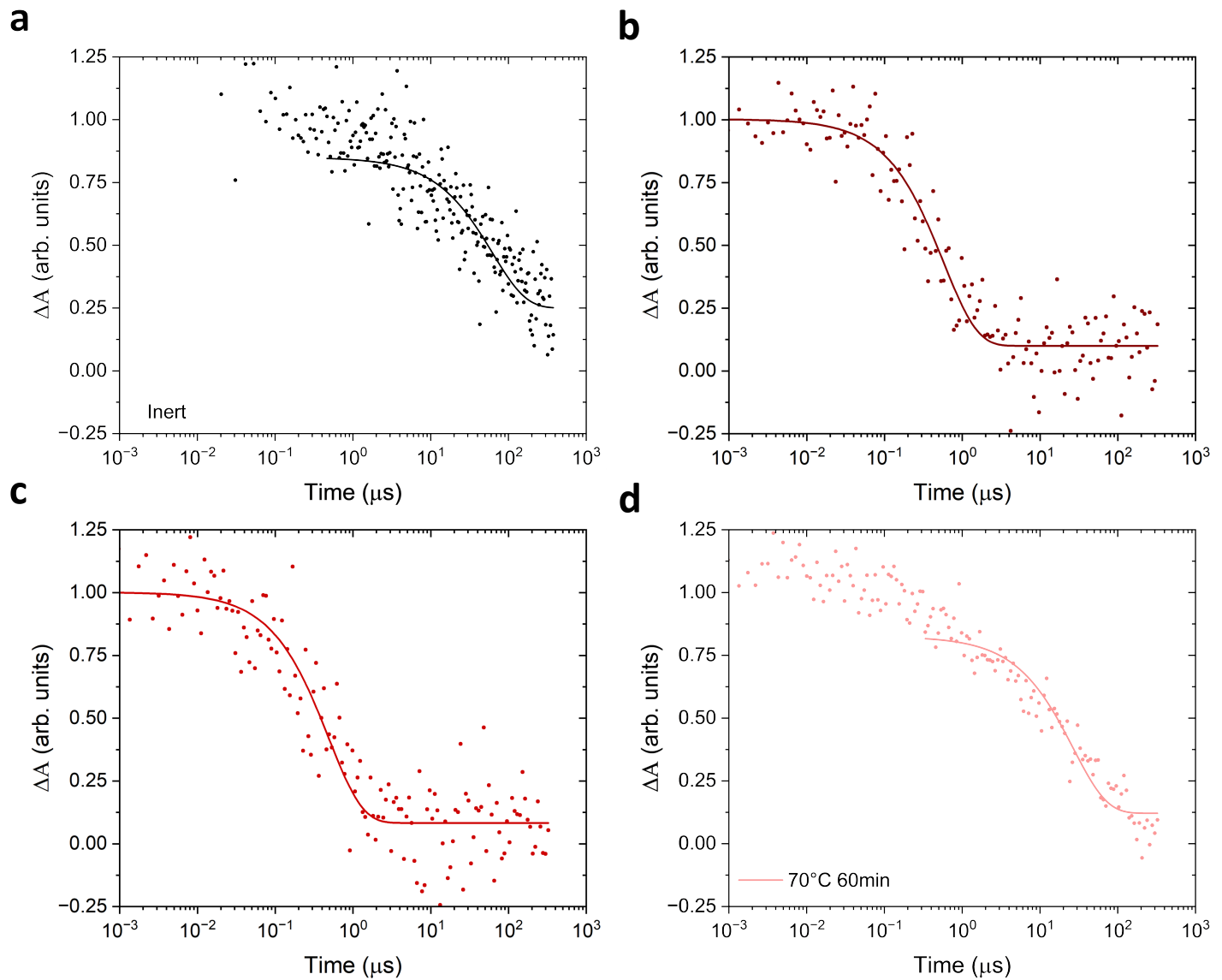


Figure S12 Transient absorption spectroscopy (TAS) for the dye in the absence of a redox mediator (a), liquid-junction solar cell (b) and after solid-state formation at 70° for 20 minutes (c) and 60 minutes (d).

1.5 Spectroscopy

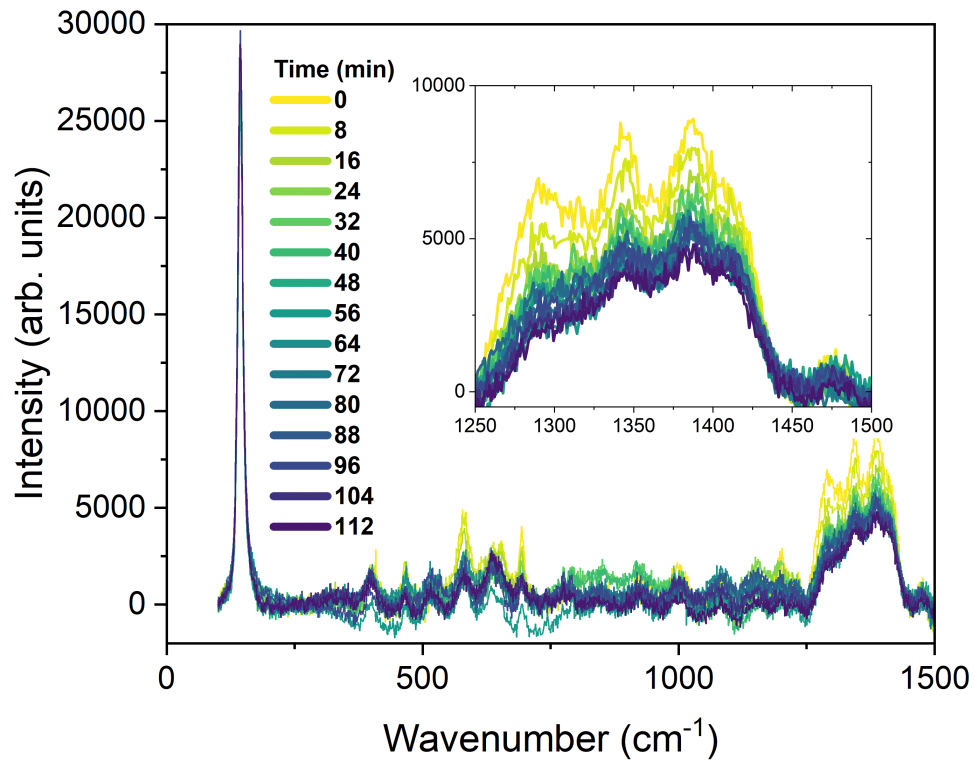


Figure S13 Time-dependent Raman spectra at probed temperature.

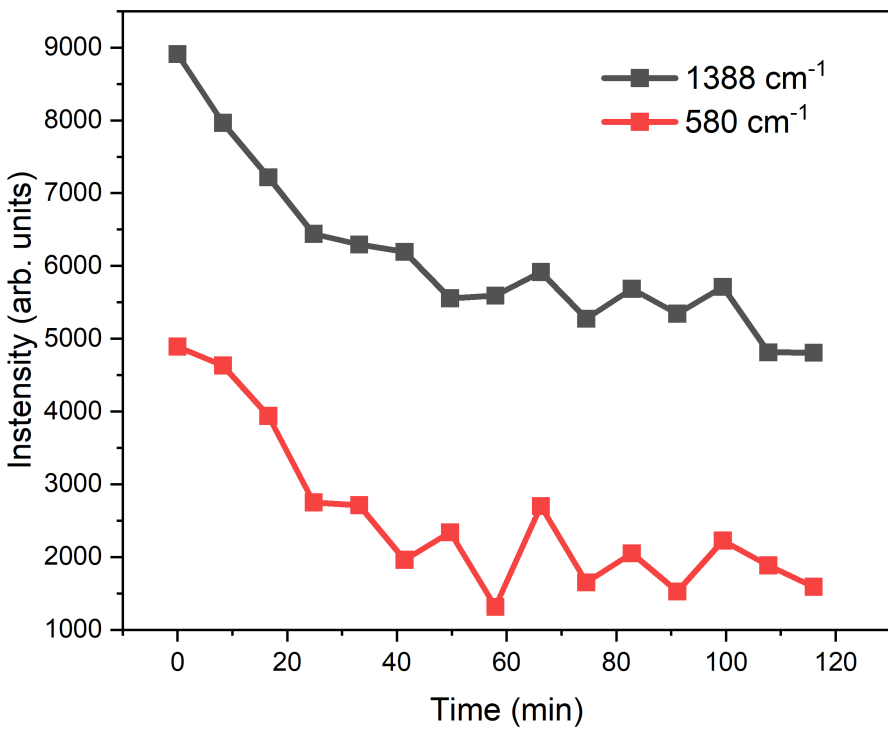


Figure S14 Raman intensity of acetonitrile CH-deformation and CCN-rocking vibration over the 120 minute solid-state formation process at $70\text{ }^{\circ}\text{C}$.

1.6 Impedance Spectroscopy

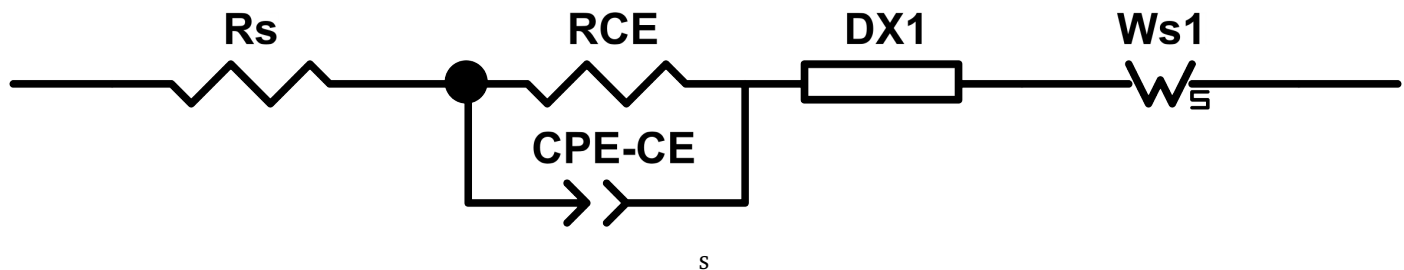


Figure S15 Equivalent circuit for electrochemical impedance spectroscopy (EIS) analysis, comprising R_s (series resistance), R_{CE} and CPE-CE (charge transfer resistance and constant phase element of the counter electrode in the high-frequency region), DX_1 (transmission line model of charge transfer resistance and capacitance at the TiO_2/HTM interface in the medium-frequency region), and W_S (Warburg diffusion element in the low-frequency region).

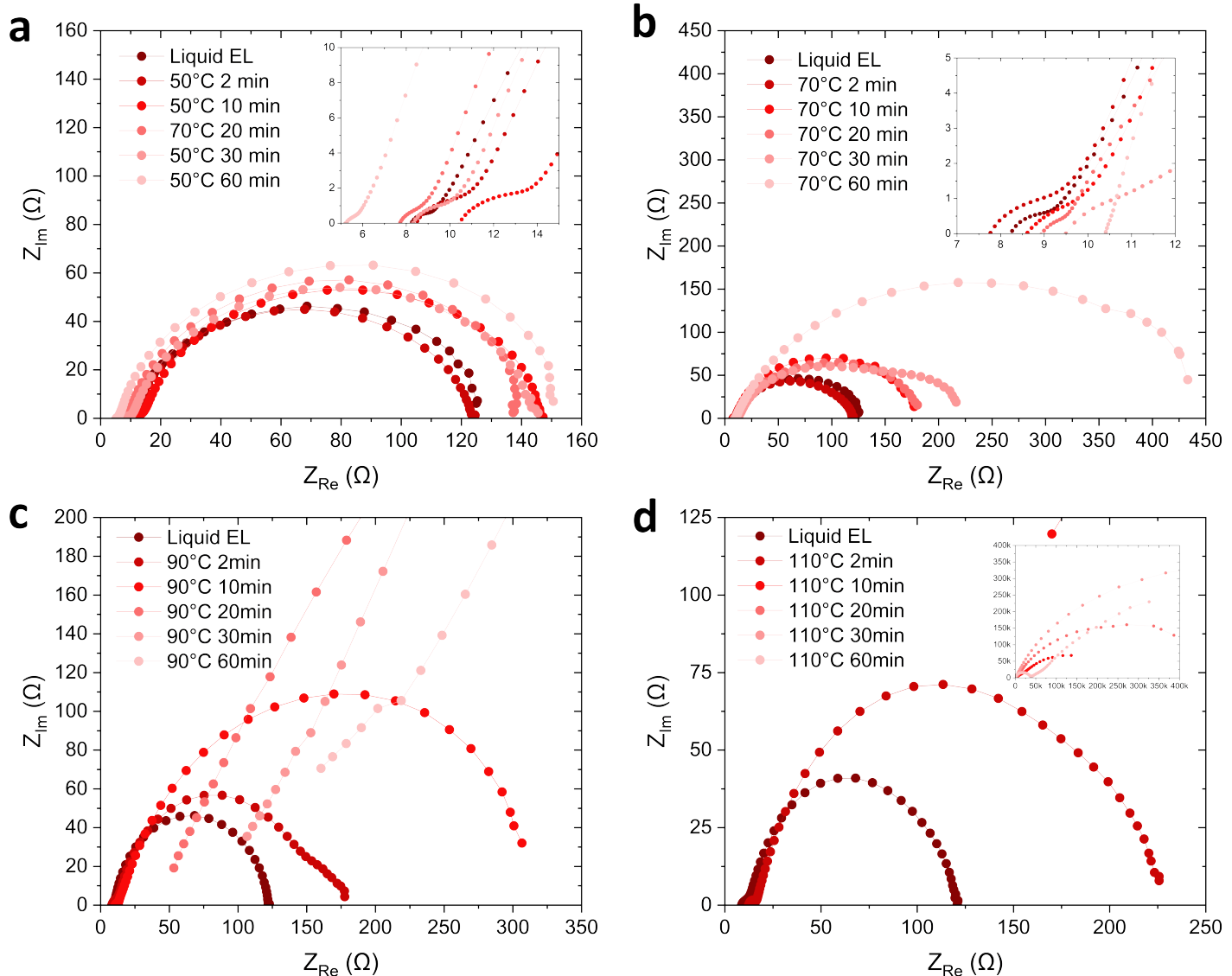


Figure S16 Electrochemical impedance spectroscopy (EIS) under dark conditions for solid-state formation at a) 50 °C, b) 70 °C, c) 90 °C and d) 110 °C for various times. The circles represent the data and solid lines the fit with the equivalent circuit displayed in S15.

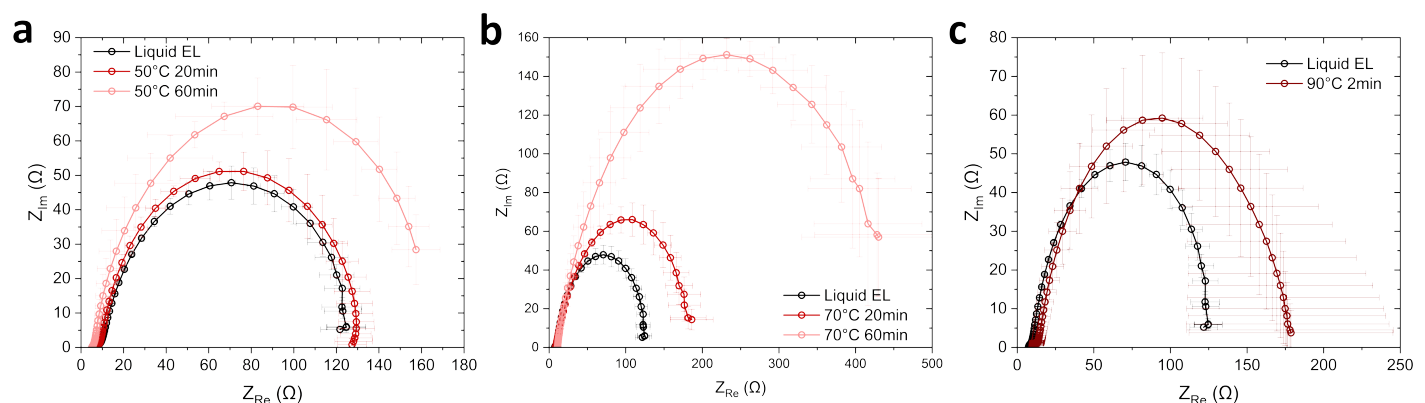


Figure S17 Uncertainty calculation for electrochemical impedance spectroscopy under dark conditions for solid-state formation at 50 °C (left), 70 °C (middle) and 90 °C (right) of selected solid-state formation conditions.

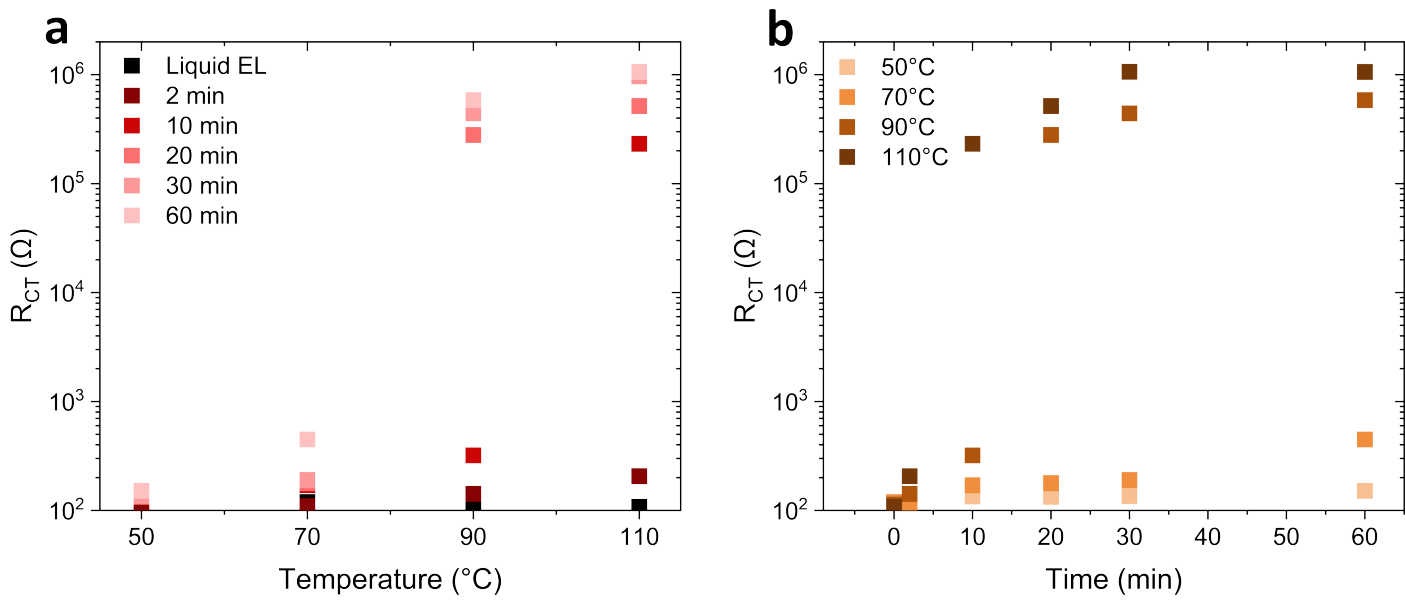


Figure S18 Charge transfer resistance at the TiO_2/HTM interface vs temperature (left) and time (right) of the solid-state formation process under dark conditions.

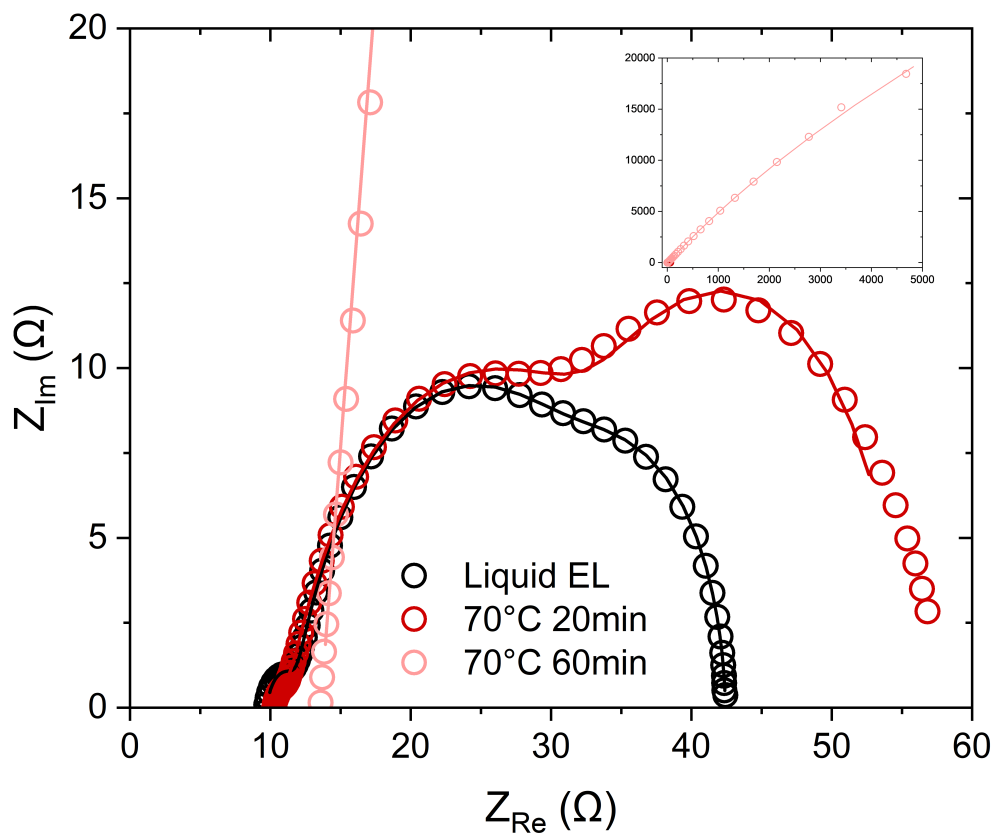


Figure S19 EIS under illumination and open-circuit potential for the solid-state formation process at 70 $^{\circ}\text{C}$.